RSC Advances

ROYAL SOCIETY OF CHEMISTRY

www.rsc.org/advances

Cite this: DOI: 10.1039/c0xx00000x

www.rsc.org/xxxxxx

Paper

Application of optical imaging technology on the *in vitro* assessment of mast cell degranulation

Shu-hua Ma[1a], Ya-nan Sun[1a], Chuan-yun Ren[b], Jing-feng Ouyang[a], Yan-ming Hou[a], Yi Wang*[a]

Received (in XXX, XXX) XthXXXXXXXXX 20XX, Accepted Xth XXXXXXXXX 20XX

DOI: 10.1039/b000000x

Mast cells are major effector cells in both IgE-mediated immune response and anaphylactoid reaction. During the process of anaphylaxis, mast cells synthesize and release inflammatory mediators from granules that induce anaphylactic symptom. Currently, *in vitro* detection methods for mast cell degranulation including colorimetric assay and morphological observation. These conventional methods are stable but have their own limitations in dynamic biological information lost, cumbersome Operating and result judgment bias. To overcome these disadvantages, we develop a new approachto observe the dynamic process of degranulation in anaphylaxis. In brief, a RBL-2H3 cell line transfected with CD63-GFP (RBL-GFP) on secretory granules was established. After activated by Compound 48/80（C48/80）, the degranulation process was observed by confocal laser scanning microscope (CLSM) within 10 min, CD63-GFP-labeled granules were traced and the maximum velocity was calculated by Imaris image processing and analysis software. Conventional colorimetric assay(β-HEX assay) and Morphological imaging method(Scanning Electron Microscopy, SEM) were selected as control methods. The results showed that the granules in RBL-2H3 cells moved faster towards plasma membrane and the number of intracellular granules significantly reduced ($P < 0.05$) after the addition of C48/80. The maximum velocity of granules was about 0.17μm/s. Furthermore, morphological changes were observed in cell and nuclear volume and pseudopodia protrusion in comparision with before treatment. Therefore, this approach is a sensitive, easy handle and low cost method which could be applied to visualize the dynamic process of mast cell degranulation *in vitro*.

Introduction

Mast cells are major effector cells in both IgE-mediated immune response and anaphylactoid reaction. During the process of anaphylaxis, mast cells synthesize and release inflammatory mediators from granules that induce anaphylactic symptom.

The degranulation process is composed by serial steps including granules transport, targeting, anchoring and fusion. Currently, *in vitro* detection methods for mast cell degranulation including colorimetric assay, which is used to detect active substances released by mast cells, such as β-hexosaminidase (β-HEX), tryptase, and histamine (1-3), and observation of morphological changes after degranulation by scanning and transmission electron microscopy (4,15,16). These conventional methods are stable but have their own limitations. Firstly, mast cell degranulation is a dynamic process, however, a series of biological information for degranulation of living cells is lost after several chemical fixations and visualization procedures were performed for detecting corresponding indicators. Secondly, many colored substances, such as some herbal extractions, interfere with the results of colorimetric assay which cause many detection errors. Finally, some of the detection methods, like electron microscopy assay, are cumbersome, complex, and expensive in sample preparation process.

Moreover, all above mentioned methods are focus on the late phase of degranulation, the consecutive morphologic changes of the individual cell, as well as the granules movement during degranulation, remain largely unclear. Therefore, a fast, simple and sensitive detection method for mast cell degranulation is urgently needed.

CD63 is a membrane surface marker located on the basophilic granule membranes in resting basophils, mast cells, and platelets. It is also known as the lysosome-associated lysosome targeting domain(9). We constructed a CD63-GFP(green fluorescent protein) plasmid and introduced it into rat basophilic leukemia (RBL-2H3) cells to observe the movements of CD63 on degranulation. Using stably transfected cell lines which express CD63-GFP on secretory granules of RBL-2H3, we investigated the relationship of naphylactoid reaction to the movement of

fluorescence granules and morphological changes after sensitized with C48/80. Our data show that the new approach is in coincident with the results of β-HEX assay and SEM. Given its visualized, dynamic and simple handle feature, it maybe a potential tool for allergen detection both in pharmaceutical factory and clinic.

Materials and Methods

Cell culture and derivation of stable transformants of RBL-GFP

RBL-2H3 cells were incubated in MEM supplemented with 10% heat-inactivated fetal bovine serum (Hangzhou Sijiqing Biological Engineering Materials Co., Ltd, China), 100 U/ml penicillin, and 100 μg/ml streptomycin. 1×10^4 RBL-2H3 cells were plated into a 35 mm glass bottom petri dish (Hangzhou Shengyou Biotechnology Co., Ltd, China) and incubated overnight at 37°C in a humidified incubator containing 5% carbon dioxide (Thermo Fisher Scientific Inc).

The transfection of CD63-GFP plasmid was performed as described in the previous work of our laboratory(5). Briefly, the whole cDNA of CD63 in RBL-2H3 cells were obtained by reverse transcription-polymerase chain reaction (RT-PCR) with the 5'primer 5'AGCTTCGAATTCATGGCGGTGGAAGGAGGAATG3' (*EcoR I*) and the 3'primer 5'ACCGGTGGATCCCGCATTACTTCATAGCCACTTCGA (*BamH I*). The pEGFG-N1 plasmid connected with CD63 cDNA by *EcoR I* and *BamH I*, then transferred the plasmid into *E. coli* DH5a, then transferred to the RBL-2H3 cells by the DNA fection kit(Tiangen, China). The RBL-2H3 cells expressed CD63-GFP plasmid were maintained in Minimum Essential Media (MEM) (Gibco) without Penicillin-streptomycin, selected in culture medium supplemented with 0.6mg/L G418(Sigma, USA) . 72 hours later, individual clones were isolated by flow cytometry and purified. Clones showing ahomogenous level of expression were selected and further subcloned by serial dilution. Cells were trypsinized every 3 days and discarded after 12 passages.

β-HEX Assays

Enzyme assays were performed on cell supernatants according tothe methods in references(6). Briefly, the RBL-GFP cells or RBL-2H3 were cultured in 96 wells culture plate and washed with Modified Tyrode's buffer(MT) (NaCl, 137 mM; KCl, 2.7mM; $CaCl_2$, 1.8 mM; $MgCl_2$, 1 mM; glucose, 5.6 mM;Hepes, 20 mM, pH 7.4; and bovine serum albumin, or BSA,0.1%) once, then incubating with MT at 37°C for 30 min. After stimulation with C48/80(10μg/ml) for 2,4,6,8,10min, cells were incubated in MT on ice for 5 min and then centrifuged at 5,000g, the supernatant was collected for enzyme activity analysis. For each well, 50 μl of supernatant were mixed with 25 μl of β-HEX in a 96-well plate(Costar, Inc.) and incubated at 37°C for 60 min. After adding termination solution (0.1M Na_2CO_3, 0.1M $NaHCO_3$, pH10.7), the plates were read on a microplate reader (Biorad, Inc.) at 405nm. The difference between RBL-GFP and RBL-2H3 in the secretion of β-HEX is also compared at 10min activated by C48/80.

The release rate of β-HEXis calculated as below:

$$\beta-\text{HEX release}=\frac{\text{concentration of }\beta-\text{HEX in supernatant}}{\text{concentration of }\beta-\text{HEX in supernatant + intracellular concentration of }\beta-\text{HEX}}\times100\%$$

Scanning Electron Microscopy (SEM)

Cells were grown on glass coverslips and after antigen stimulation were fixed for 1 hour in 4% glutaraldehyde in 100-mmol/L phosphate buffer at pH 7.4. Samples were fixed for 1 hours in osmic acid and washing by 1 mol/L phosphate buffer for 3 times, then gradually dehydrate dusing increasing concentrations of ethanol and then critical point dried with CO_2 and gold sputtering (E1010, Hitachi, Japan). The samples were observed in a Hitachi S3400N scanning electron microscope at 5 kV.

Observation of Intracellular granules movement of RBL-GFP

2ml RBL-GFP dilution (1×10^6/ml) were cultured 24 hrs in a 35mm glass bottom Petri dish for the experiment. Real-time monitoring of granule movement during mast cell degranulation was observed with CLSM(FV-1000, OLYMPUS, Japan). The parameters for the optical imaging were the following: 512 x 512 pixels and 12-bit intensity resolution. The objective was 100 × oil immersion(NA 1.45). Green fluorescent protein (GFP) was excited at 488 nm, with laser intensity at 0.8%, 10 seconds per frame for 10min after activation with C48/80. As the observation interval on RBL-GFP is 10min, the effect of laser irradiation on cell viability was observed on rested RBL-GFP in parallel with administration groups.

All data were processed with Auto Quant (version X2.1.3) and analysed with Imaris processing software.

Simultaneous Observation of and morphological changes of RBL-GFP

In order to see the morphological changes of cell, cultured cells were loaded with 1μM Calcein-AM(for cytoplasm) and 0.5 g/ml Hoechst 34580(for the nucleus). After loaded at 37°C for 30 min, cells were observed with CLSM at 350nm(Calcein-AM), 488nm(GFP) and 515nm(Hoechst 34580) simultaneously. 100 × oil immersion objective (NA 1.45) was used and 5μm steps in the Z-axial direction to make 3D-fluorescence imaging before (0 min) and after (5,10 min) mast cell degranulation.

All data were processed with Auto Quant (version X2.1.3) and analysed with Imaris processing software.

Image analysis

Imaris 7.4.0 software (Bitplane, Switzerland) was used for fluorescence image analysis. 2D track module of Imaris was used to track movement speed of fluorescent granules.

The surface measurement module was used for reconstruction of three-dimensional structures of granules, nucleus, and the cytoplasm.

Statistical analysis

All experiments were performed at least three times. All data are expressed as mean±SD. The significance of the difference between samples and control groups was analysed by t-test.

Results

Detection of β-HEX released from sensitized RBL-GFP

To characterize the ability of RBL-GFP, β-HEX release was used to verify that transfected cells still had normal function of mast cell degranulation. The result show that 2min after being treated with C48/80(10μg/ml), the release of β-HEX could be detected and continue to increase with dose-dependent manner until 10min (Fig 1A), while negative control group showed no obvious changes.

Moreover, the release of β-HEX from RBL-2H3 cells and RBL-GFP was compared after being activated with C48/80 for 10min （Fig.1B）. The result showed that RBL-GFP behaved similarity with normal RBL-2H3 cell line which means the transfection did not affect the degranulation character of RBL-GFP.

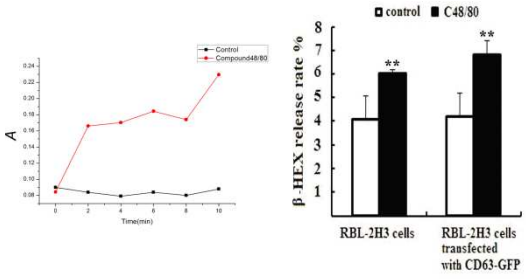

Fig.1 β - HEX release of RBL-GFP stimulated by C48/80.

To characterize the ability of RBL-GFP, β-HEX release was used to verify that transfected cells still had normal function of mast cell degranulation. (A) RBL-GFP,treated with compound 48/80 at 10μg/ml for 2,4,6,8,10 min. β - HEX release was determined by colorimetric assay. Negative control was treated with same volume of saline. (B) β-HEX release rate of RBL-2H3 and RBL-GFP after being activated with C48/80 at 10μg/ml for 10min. n=3, mean ±SD ***P<0.01vs.* control

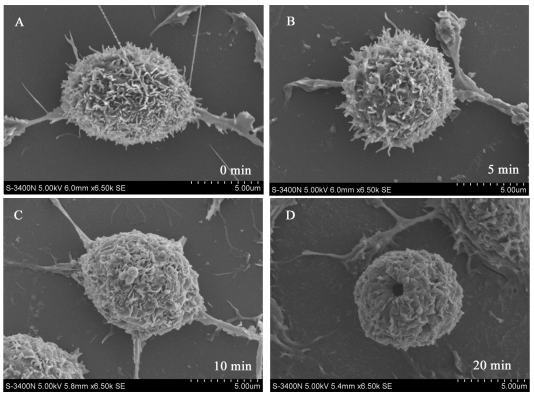

Fig.2 Morphological changes of RBL-GFP cells stimulated with C48/80.

Cells were then fixed and processed for SEM and observed at 5KV, ×6500(see method). (A) The microvillous dorsal surface of unstimulated RBL-GFPcells that spread and formed multiple membrane ruffles in response to antigen stimulation. (B) and (C) RBL-GFP cell had lost a lot of its surface protrusions 5-10min after stimulation (D) cells rounded up and membranous retract could be observed (a big hole appears) after stimulation for 20min.

Morphological changes of RBL-GFP cells observed by SEM.

Control RBL-2H3 cell exhibited a heterogeneous display of membranous ridges (Fig 2*A*). When the cells are stimulated with C48/80 (10μg/ml), they are not activated in asynchronized manner—i.e., the amounts of time that it takes for the individual cells to undergo exocytosis and recovery differ. Therefore, the cells were at different degranulation and recovery stages (Fig 2 *B-D*). In Fig 2*B* and *C*, a RBL-GFP cell had lost a lot of its surface protrusions 5-10min after stimulation. These protrusions could contain its intracellular granules, in as much as it has been suggested that granule-plasma membrane fusions can be observed during exocytosis. In Fig 2*D*, the cell that probably undergo intermediate stages of mast cell degranulation are shown; retracted membranous hole are present.

Analysis of the quantity and velocity of granules during mast cell degranulation

Many different sizes of granules with a diameter ranging from 0.46 μm to 1.78 μm were observed (Fig. 3B). Uniform green fluorescence was expressed in granule membranes of RBL-GFP, and movement changes of fluorescent granules were dynamically tracked by the CLSM. In resting cells, 80% of granules did not move or only did irregular Brownian movements, with a speed of only $(2.0 \pm 0.2)\times10^{-2}$μm/s. Only 20% of granules moved fast along the longitudinal axis of a pseudopodium. During degranulation, granules moved gradually towards plasma membrane with a maximum speed of up to $(17.0 \pm 0.5) \times10^{-2}$μm/s (Fig.3A), and the number of granules was decreased from $(1.76 \pm 0.13)\times10^{2}$ to $(1.38 \pm0.08)\times10^{2}$ (Fig. 3C). Many granules deviated from the focal plane, or fused into a larger one for extra cellular secretion.

In order to exclude the laser radiation damage on cells during the observation, a parallel observation of CLSM was conducted on resting RBL-GFP cells. The results showed that after a continuous observation, cells were alive without shrinkage and death under the scanning condition for 10 minutes (Fig3D). The experimental conditions did not affect cell morphology.

Changes of cell 3-D structure after mast cell degranulation

Reconstruction of 3-D structure was performed after scanning of optical sections of mast cells. Surface renderings of cytoplasm, nucleus, and granules were processed by Imaris (Fig.4A) and results were obtained using corresponding algorithms of Imaris.

A newly formed Pseudopodia protrusion was observed after degranulation (Fig. 4B, red box), which was easily ignored without rendering.

As was shown in Fig. 4C, after mast cell degranulation, the cell surface area was increased from $(2.1\pm 0.5) \times10^{3}$ μm square to $(4.5\pm 1.1)\times10^{3}$ μm square , which was expanded 1.12 times as

that before degranulation. Cell volume was expanded from (2.5 ± 0.3) $\times 10^3$μm cubic to (2.8 ± 0.3) $\times 10^3$μm cubic, with an increase of 12.2%. Nuclear surface area was decreased from (4.7 ± 0.9) $\times 10^2$μm square to (3.9 ± 0.6) $\times 10^2$μm square, with a 17% reduction. Nuclear volume was reduced from (4.8 ± 1.0) $\times 10^2$ μm cubic to (4.3 ± 1.0) $\times 10^2$ μm cubic, which was reduced by 11.8%. Thus, morphological changes in cell surface, cell volume, nuclear could be recognized after mast cell degranulation.

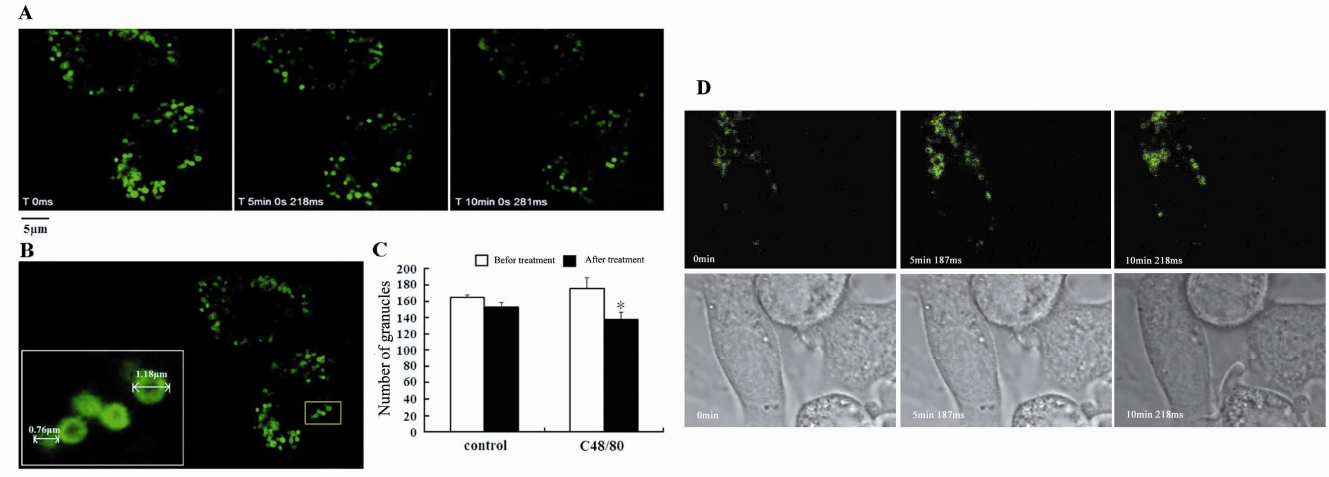

Fig.3Movement analysis of secretory granules after being stimulated with Compound 48/80 in RBL-GFP cells and cell viability detection of RBL-GFP Scanning with CLSM system A: Time-lapse confocal images of secretory granules at 0, 5, 10 min after being stimulated with C 48/80 (10μg/ml). The maximum velocity of granules was about 0.17μm/s and the number of granules was decreased compared with 0min; B: The diameter ranging of granules was from 0.46 μm to 1.78 μm; C: Granules counting in RBL-2H3 cells before (white bar) and after degranulation treated with compound 48/80 (black bar). All data points represent the mean±SD of measurements made in quadruplicate.*$P<0.05$ *vs.* values before degranulation; D: The cell state no significant change after a continuous observation for 10 min (488 nm, ×100 oil immersion lens, sampling rate 12.5μs / pixels, laser intensity 0.8%).

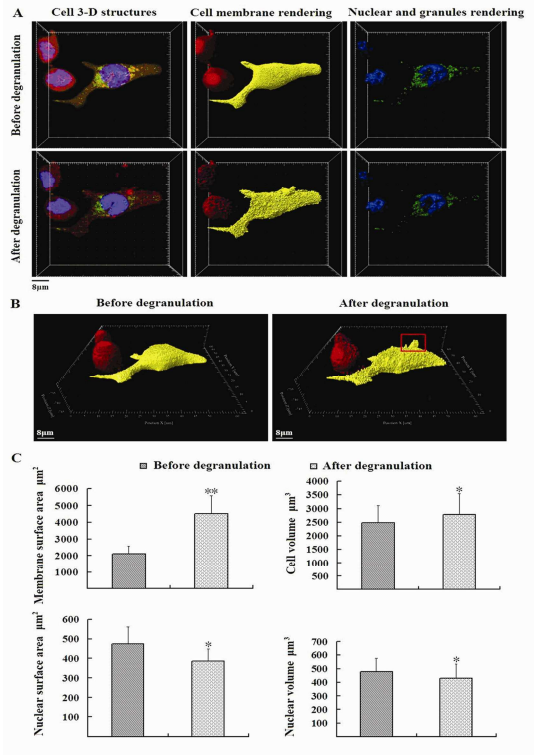

Fig.4 Morphological changes in RBL-GFP cells stimulated by C48/80

A: 3-D construction and surface rendering of RBL-GFP cells loaded with Hoechst 34580 and volumetric indicator Calcein-AM. Morphological changes of cell surface area, cell volume and nuclear were observed before and after mast cell degranulation. Blue: nuclear, Yellow: cell membrane, Green: secretory granules; B: Newly formed Pseudopodia protrusion (red box in right panel) was observed after C48/80-induced degranulation; C: The surface and nuclear changes of RBL-GFP measured by Imaris before and after degranulation. n=6, mean±SD.*$P<0.05$, **$P<0.01$ *vs.* control

Discussion

Traditional Chinese medicine (TCM) injection is a new formulation from China. There are more than 70 kinds of TCM injection from 1950s. It has been widely used in clinic in for several decades and tested to be effective in China. However, in recent years, as production and quality control reasons, security incidents occurred frequently. It was reported that 60% of the adverse effects are anaphylactoid reaction (7). In view of allergic reaction dangerous, people increasingly aware of the importance of early prevention. Hence, early rapid diagnosis for allergic reaction is one of the best tools for reduce adverse effect of TCM injections.

Colorimetric assay and morphology detection are main detection methods for *in vitro* mast cell degranulation. Usually, we use end point colorimetric assay to detect the release of β -HEX, tryptase, histamine to determine antigens for mast cell degranulation. As the detection wave length is usually 405nm, it is always be problems for the research of herbal medicine, because dark color substances from herbal medicine covered the spectrum from 400-500nm, this may interfere with the results of colorimetric assay which cause many detection errors. Therefore, it greatly limited the application of colorimetric assay in TCM safety control.

SEM is a typical mophorlogy detection method. To get good images, samples need fixation, dehydration and dryness with critical point drier. However, mast cell degranulation is a dynamic process, a series of biological information for degranulation of living cells is lost after aseries of activities. Moreover, some reagents used in SEM, like osmic acid, is toxity

and expensive.

The early stage of mast cell degranulation consists of a series of steps, including transportation, orientation, and anchoring of granules as well as their integration with the plasma membrane. Each step is strictly regulated (8). Thus to observe the movement of granules and monitor the membrane integration process directly is the most reliable and simple method.

In our previous study, RBL-2H3 cells that stably expressed CD63-GFP was established by plasmid transfection and secretory granules were directly visualized during degranulation. As excitation wave length of GFP is 488nm and emission at 507nm, it can be successfully avoid the disturb of dark color of herbal extraction and TCM injection, so it is suitable for the allergen tracing research in TCM injection.

In this study, the dynamic changes of secretory granules and extraction of characteristic parameters of RBL-2H3 cells after degranulation were further focused on. Movement speed of CD63-GFP labeled granules were dynamically increased in degranulation. Therefore, we can judge mast cell degranulation only from the movement speed of granules, and access the risks of anaphylactoid reaction. It is simple and low cost.

The results showed that during mast cell degranulation, morphological changes such as increased cell surface area, expanded cell volume, nuclear condensation, and reduced nuclear volume were observed, which is important to determine anaphylactoid reaction.

It was observed in this study that in resting cells, most granules nearly did not move or only did irregular Brownian movements. While in cells with degranulation, granules moved gradually towards plasma membrane and within 10min many granules deviated from the focal plane, resulting in reduced number of granules in the focal plane. Similarly to the findings of Amano T(10), we also observed that in mast cells without degranulation, a small part of granules moved fast along the longitudinal axis of a pseudopodium. Studies have shown that the long-distance movement and exocytosis of CD63 labeled secretory granules depended on microtubule assembly and activity of protein kinase C(11-13). However, the translocation of some recycling endosomes to the plasma membrane depended neither on protein kinase C(14), nor on microtubule aggregation. So our next focus is microtubule rearrangement and its downstream signal transduction regulation of secretory granules or space targeting of other endosomes.

Conclusions

In this study, optical imaging technology was applied to study the dynamic process of mast cell degranulation and images collected were qualitatively and quantitatively analyzed with Imaris software. Thus a new approach for rapid *in vitro* assessment of mast cell degranulation was created. Characteristic changes of mast cell degranulation were described from the aspects of dynamic changes of secretory granules, increased cell surface area after degranulation, nuclear condensation, and pseudopodia protrusion. Data of mast cell degranulation were dynamically obtained with multiple parameters, which overcame the deficiencies of the conventional methods. It will provide a new method for screening for allergens in drug safety evaluation, allergen detection in clinic. Further work will carry on in qualitative and quantitative analysis.

Notes and references

[a]*Beijing Key Laboratory of TCM Basic Research on Prevention and Treat ment of Major Disease, Experimental Research Center，China Academy of Chinese Medical Sciences，Beijing，China.*

[b]*Dongzhimen Hospital , Beijing University of Chinese Medicine, Beijing , China.*

[1]These authors contributed equally to the work.

*Correspondece to: Wang Yi, Experimental Research Center， China Academy of Chinese Medical Sciences，Beijing，China.

Fax:+86-01-64024477 ; Tel:+86-01-64014411-2560 ;

E-mail:wangyi02@tsinghua.org.cn

‡This work is supported by Project supported by the National Natural Science Foundation of China No.81373884. Basic scientific research fund from Ministry of Fina e of China No.ZZ2011010, No.ZZ2011011. National Natural Science Foundation of Beijing,China No. 7132157.

1 Li J, Jin J, Guan CW, Li P, Tu JS, Sun HM and Huang ZY. Study of degranulation in mast cell RBL-2H3 induced by Tween 80. Drug Evaluation Research, 2010, (005):379-383.

2 Wang W, Zhou Q, Liu L and Zou K.. Anti-allergic activity of emodin on IgE-mediated activation in RBL-2H3 cells. Pharmacol Rep. 2012, 64(5):1216-22.

3 Hagenlocher Y1, Bergheim I, Zacheja S, Schäffer M, Bischoff SC, Lorentz A. Cinnamon extract inhibits degranulation and de novo synthesis of inflammatory mediators in mast cells.Allergy. 2013, 68(4):490-7.

4 Zhu L, Lu HM, Yu CX, He XL and Su DH. Observation on anti-IgE antibody-induced mast cell degranulation by electron microscopy. Chin J Immunol, 2002, 18(5):357-357.

5 Hu JJ, Hou YM, Zhang Q, Lei HT, Wang Y and Wang DQ. Real-time detection of mast cell degranulation in anaphylactoid reaction. China Journal of Chinese Materia Medica, 2011,36(14):1860-1860.

6 Wang W, Zhou Q, Liu L and Zou K. Anti-allergic activity of emodin on IgE-mediated activation in RBL-2H3 cells. Pharmacological Reports, 2012, 64(1216):1216-1222.

7 Zhang HF, Zhai CK and Zheng YZ, advancement of experimental studies on sensitization research of Traditional Chinese Medicine Injection. Chinese Journal of Experimental Traditional Medical Formulae.2010,16(10):204-206

8 Liu DF, Zhang CG and wu JM. Study on mechanisms of mast cell degranulation. Sect Clin Biochem & Lab Med Foreign Med Sci, 2004,25(2):137-139.

9 Levy S and Shoham T. The tetraspanin web modulates immune-signalling complexes. Nature Reviews Immunology, 2005, 5(2):136-148.

10 Amano T, Furuno T, Hirashima N, Ohyama N and Nakanishi M. Dynamics of intracellular granules with CD63-GFP in rat basophilic leukemia cells. Journal of Biochemistry, 2001, 129(5):739-744.

11 Nishida K, Yamasaki S, Ito Y, Kabu K, Hattori K, Tezuka T, Nishizumi H, Kitamura D, Goitsuka R and Geha RS. FcεRI-mediated mast cell degranulation requires calcium-independent microtubule-dependent translocation of granules to the plasma membrane. The Journal of cell biology, 2005, 170(1):115-126.

12 Blank U and Rivera J. The ins and outs of IgE-dependent mast-cell exocytosis. Trends in immunology, 2004, 25(5):266-273.

13 Naal RMZ, Holowka EP, Baird B and Holowka D. Antigen□Stimulated Trafficking from the Recycling Compartment to the Plasma Membrane in RBL Mast Cells. Traffic,2003,4(3):190-200.

14 Wu M, Baumgart T, Hammond S, Holowka D and Baird B. Differential targeting of secretory lysosomes and recycling endosomes in mast cells revealed by patterned antigen arrays. Journal of cell science, 2007, 120(17):3147-3154.

15 DemoSD, MasudaE, RossiAB, ThrondsetBT, GerardAL,Chan EH, ArmstrongRJ,FoxBP, LorensJB, PayanDG,Scheller RH and FisherJM.Quantitative measurement of mast cell degranulationusing a aovel flow cytometric annexin-Vbinding assay.Cytometry, 1999, 36(4):340-8.

15 Xiang Z, Block M, Löfman C and Nilsson G.IgE-mediated mast cell degranulation and recovery monitored by time-lapse photography.J Allergy Clin Immunol, 2001, 108(1):116-21.